High-pressure Synthesis, Crystal Structure, and Properties of δ-Ce(BO$_2$)$_3$

Almut Haberer, Gunter Heymann, and Hubert Huppertz

Department Chemie und Biochemie, Ludwig-Maximilians-Universität München,
Butenandtstraße 5 – 13 (Haus D), 81377 München, Germany

Reprint requests to H. Huppertz. E-mail: huh@cup.uni-muenchen.de

The cerium *meta*-oxoborate δ-Ce(BO$_2$)$_3$ was synthesized under high-pressure / high-temperature conditions of 3.5 GPa and 1050 °C in a Walker-type multianvil apparatus. The crystal structure was determined by single crystal X-ray diffraction data, collected at r. t. The compound crystallizes monoclinicly in the space group $P2_1/c$ with the lattice parameters $a = 422.52(8)$, $b = 1169.7(2)$, $c = 725.2(2)$ pm, and $\beta = 91.33(3)°$. The structure is isotypic to the recently published high-pressure phase δ-La(BO$_2$)$_3$, consisting exclusively of corner sharing [BO$_4$]$^{5-}$ tetrahedra.

Key words: High-pressure Phase, Borate, Crystal Structure, Multianvil

Introduction

Recent investigations into the chemistry of oxoborates under high-pressure / high-temperature conditions led to a large variety of new compositions and polymorphs. Compounds like $RE_4B_6O_{15}$ (RE = Dy, Ho) [1 – 3] and α-$RE_2B_4O_9$ (RE = Sm–Ho) [4 – 6] have extended the structural chemistry of oxoborates by the new structural motive of edge-sharing [BO$_4$]$^{5-}$ tetrahedra. The oxoborates $RE_3B_5O_{12}$ (RE = Tm–Lu) [7] and β-HfB$_2$O$_5$ [8], formed under high pressure, showed structures analogous to those found in silicate chemistry. With the synthesis of β-HfB$_2$O$_5$ [8] and β-SnB$_4$O$_7$ [9], we were able to obtain the first crystalline compounds in the ternary systems Hf-B-O and Sn-B-O, respectively. Normally, these systems form glasses at ambient-pressure conditions, while the parameter pressure induces crystallization in both systems. Furthermore, we observed the existence of several new polymorphs of well-characterized normal-pressure phases, *e. g.* χ-REBO$_3$ (RE = Dy, Er) [10], β-CaB$_4$O$_7$ [11], β-HgB$_4$O$_7$ [12], and β-ZnB$_4$O$_7$ [13]. Synthetic investigations into the technologically important non-centrosymmetric material α-BiB$_3$O$_6$ (BIBO) revealed two new centrosymmetric polymorphs (β-BiB$_3$O$_6$ and γ-BiB$_3$O$_6$ [14]) and a non-centrosymmetric high-pressure modification δ-BiB$_3$O$_6$ showing a remarkable SHG effect [15]. In analogy to BiB$_3$O$_6$, which exhibits four different modifications, we were also able to add a third and a fourth structural variant to the rare earth *meta*-oxoborates RE(BO$_2$)$_3$ $\equiv$ REB$_3$O$_6$. Following the well-known monoclinic phases α-RE(BO$_2$)$_3$ [16 – 29] and the orthorhombic phases β-RE(BO$_2$)$_3$ [30, 31], we were able to add a third polymorph γ-RE(BO$_2$)$_3$ (La–Nd) [32, 33] to the system under high-pressure conditions (7.5 GPa). A more detailed investigation of the pressure region between ambient pressure and 7.5 GPa led to the discovery of a fourth *meta*-oxoborate δ-La(BO$_2$)$_3$ at a pressure of 5.5 GPa [34]. A detailed summary concerning the structures of all four modifications is given in reference [34]. With δ-Ce(BO$_2$)$_3$ we present the second example of the fourth modification of rare earth *meta*-oxoborates, about which we report the synthetic conditions, structural details, thermal behaviour, and IR spectra, in comparison to the already known phase δ-La(BO$_2$)$_3$.

Experimental Section

The new modification of cerium *meta*-oxoborate was synthesized under high-pressure / high-temperature conditions of 3.5 GPa and 1050 °C. Starting reagents were powders of CeO$_2$ (Auer-Remy, Hamburg, Germany, 99.9 %) and B$_2$O$_3$ (Strem Chemicals, Newburyport, USA, 99.9 %), which were carefully mixed and filled into a boron nitride crucible (Henze BNP GmbH, HeBoSint®, Kempten, Germany) in the stoichiometric ratio CeO$_2$: B$_2$O$_3$ = 2 : 3. According to eq. (1), the products of this redox reaction were δ-Ce(BO$_2$)$_3$ and oxygen.
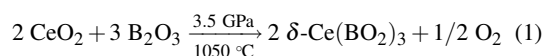
$$2\,\text{CeO}_2 + 3\,\text{B}_2\text{O}_3 \xrightarrow[1050\ \text{°C}]{3.5\ \text{GPa}} 2\,\delta\text{-Ce(BO}_2)_3 + 1/2\,\text{O}_2 \quad (1)$$

Table 1. Crystal data and structure refinement details for δ-Ce(BO$_2$)$_3$.

Empirical formula	Ce(BO$_2$)$_3$ ($\equiv$ CeB$_3$O$_6$)
Molar mass, g $\cdot$ mol^{-1}	268.55
Crystal system	monoclinic
Space group	$P2_1/c$ (No. 14)
Powder diffractometer	Stoe Stadi P
Radiation	Cu$K_{\alpha1}$ (λ = 154.06 pm)
Powder diffraction data	
a, pm	423.29(2)
b, pm	1170.97(6)
c, pm	725.87(4)
β, deg	91.30(1)
Volume, Å^3	359.69(2)
Single crystal diffractometer	Stoe-IPDS
Radiation	MoK_α (λ = 71.073 pm)
Single crystal data	
a, pm	422.52(8)
b, pm	1169.7(2)
c, pm	725.2(2)
β, deg	91.33(3)
Volume, Å^3	358.3(2)
Formula units per cell	Z = 4
Temperature, K	293(2)
Calculated density, g $\cdot$ cm^{-3}	4.98
Crystal size, mm^3	$0.12 \times 0.06 \times 0.03$
Detector distance, mm	45.0
Irradiation exposure, min	14
Number of exposures	200
Absorption coefficient, mm^{-1}	12.6
$F(000)$, e	484
θ range, deg; hkl range	$3.31 - 31.57$; ±6, $-16/+17$, ±10
Total no. reflections	4583
Independent reflections	1153 (R_{int} = 0.0276)
Reflections with $I \geq 2\sigma(I)$	946 (R_σ = 0.0199)
Data/parameters	1153/92
Transm. ratio (min/max)	0.516/0.677
Goodness-of-fit (F^2)	0.974
Final R indices [$I \geq 2\sigma(I)$]	R_1 = 0.018, wR_2 = 0.043
R Indices (all data)	R_1 = 0.024, wR_2 = 0.045
Extinction coefficient	0.006(1)
Larg. diff. peak and hole, e $\cdot$ Å^{-3}	0.76/$-$0.86

Table 2. Atomic coordinates (*Wyckoff* site 4*e* for all atoms) and isotropic equivalent displacement parameters (U_{eq}, Å^2) for δ-Ce(BO$_2$)$_3$ (space group: $P2_1/c$). U_{eq} is defined as one third of the trace of the orthogonalized U_{ij} tensor.

Atom	x	y	z	U_{eq}
Ce	0.21780(4)	0.37691(2)	0.88148(2)	0.00572(8)
B1	0.6875(8)	0.3785(3)	0.5727(5)	0.0047(5)
B2	0.8060(8)	0.5936(3)	0.6262(4)	0.0046(6)
B3	0.6762(9)	0.3339(3)	0.2115(5)	0.0049(5)
O1	0.8449(5)	0.3737(2)	0.3898(3)	0.0047(4)
O2	0.7928(6)	0.4763(2)	0.6839(3)	0.0059(4)
O3	0.3473(5)	0.3796(2)	0.5481(3)	0.0057(4)
O4	0.7461(6)	0.4096(2)	0.0603(3)	0.0065(4)
O5	0.7817(6)	0.2843(2)	0.6940(3)	0.0071(4)
O6	0.6702(6)	0.6691(2)	0.7643(3)	0.0051(4)

could be easily separated from the boron nitride crucible as a colourless, air- and water-resistant, crystalline solid.

In order to define the pressure range in which this δ-modification of cerium *meta*-oxoborate can be synthesized, additional experiments under varying pressure conditions and at the same temperature were performed. Pressure conditions of 2 GPa led to the synthesis of the cerium *ortho*-oxoborate π-CeBO$_3$ [24, 39, 40] and a hitherto unknown by-product. Slightly higher pressure of 3 GPa resulted in the formation of a glass. At 5.5 GPa, the densest modification of the rare earth *meta*-oxoborates was formed: γ-Ce(BO$_2$)$_3$. Obviously, there exists only a small pressure range ($3.5 - 4.5$ GPa) in which δ-Ce(BO$_2$)$_3$ can be successfully synthesized.

Crystal structure analysis

The powder diffraction data of monoclinic δ-Ce(BO$_2$)$_3$ were collected with a Stoe Stadi P diffractometer, using monochromatized Cu$K_{\alpha1}$ radiation. The diffraction pattern of δ-Ce(BO$_2$)$_3$ was indexed with the program ITO [41] on the basis of a monoclinic unit cell. The lattice parameters a = 423.29(2), b = 1170.97(6), c = 725.87(4) pm, and β = 91.30(1)° (Table 1) were obtained from least-squares fits of the powder data. The correct indexing of the pattern was confirmed by intensity calculations [42], taking the atomic positions from the structure refinements of δ-Ce(BO$_2$)$_3$ (Table 2). The lattice parameters determined from the powder and the single crystal data [a = 422.52(8), b = 1169.7(2), c = 725.2(2) pm, and β = 91.33(3)°] agree well.

Small single crystals of δ-Ce(BO$_2$)$_3$ were isolated by mechanical fragmentation and examined by Buerger precession photographs. Single crystal intensity data were collected at r. t. from a regularly brick-shaped colourless crystal by use of a Stoe IPDS-I diffractometer (MoK_α radiation, λ = 71.073 pm). A numerical absorption correction (HABITUS [43]) was applied to the intensity data. All relevant information concerning the data collection is listed in Table 1. The starting positional parameters were taken from the structural refinement of δ-La(BO$_2$)$_3$ [34]. The structure of δ-

High-pressure conditions were applied using multianvil equipment, based on a Walker-type module and a 1000 t press (both devices from the company Voggenreiter, Mainleus, Germany). The boron nitride crucible was positioned inside of the centre of an 18/11 assembly, which was compressed by eight tungsten carbide cubes (TSM-10, Ceratizit, Reutte, Austria). For a detailed description of the assembly, see references [35 – 38].

In order to synthesize δ-Ce(BO$_2$)$_3$, the crucible was compressed up to 3.5 GPa in 90 min. At constant pressure, the sample was heated up to 1050 °C in 20 min (cylindrical graphite furnace), kept at this temperature for 5 min, and cooled down to 450 °C within another 30 min. Afterwards, the sample was quenched to r. t. by switching off the heating. A decompression period of 5 h followed. δ-Ce(BO$_2$)$_3$

Atom	U_{11}	U_{22}	U_{33}	U_{23}	U_{13}	U_{12}
Ce	0.0048(2)	0.0075(1)	0.0048(1)	−0.00061(6)	−0.00014(6)	−0.00059(6)
B1	0.002(2)	0.006(2)	0.006(2)	−0.001(2)	0.000(2)	−0.000(1)
B2	0.005(2)	0.005(2)	0.004(2)	−0.0014(9)	0.000(2)	−0.003(1)
B3	0.004(2)	0.007(2)	0.004(2)	−0.001(1)	0.002(2)	0.001(1)
O1	0.0023(9)	0.0089(9)	0.0029(9)	−0.0017(7)	0.0003(7)	−0.0002(7)
O2	0.01(2)	0.0028(9)	0.0052(9)	0.0009(7)	−0.0009(8)	−0.0001(7)
O3	0.003(1)	0.0087(9)	0.0052(8)	0.0015(7)	0.0009(7)	−0.0006(7)
O4	0.006(2)	0.0059(8)	0.008(1)	0.0029(7)	0.0019(8)	−0.0006(7)
O5	0.006(2)	0.0064(9)	0.009(1)	−0.0001(7)	−0.0024(8)	−0.0017(7)
O6	0.004(1)	0.0065(8)	0.0053(9)	−0.0008(7)	−0.0006(8)	0.0001(7)

Table 3. Anisotropic displacement parameters (U_{ij}, Å²) for δ-Ce(BO₂)₃ (space group $P2_1/c$).

Ce–O4a	243.3(3)	B1–O3	144.4(4)	B2–O2	143.6(4)	B3–O4	144.6(4)
Ce–O3a	249.1(2)	B1–O5	145.9(4)	B2–O3	144.2(4)	B3–O5	145.9(4)
Ce–O5a	251.0(2)	B1–O2	146.3(4)	B2–O6	146.3(4)	B3–O6	147.8(5)
Ce–O4b	253.6(2)	B1–O1	149.9(4)	B2–O1	153.1(4)	B3–O1	153.4(4)
Ce–O2a	255.1(2)						
Ce–O4c	258.4(2)		∅ 146.6		∅ 146.8		∅ 147.9
Ce–O6a	265.6(2)						
Ce–O6b	269.7(2)			O1–B1	149.9(4)		
Ce–O5b	297.5(3)			O1–B2	153.1(4)		
Ce–O2b	307.7(2)			O1–B3	153.4(4)		
Ce–O3b	327.6(3)						
Ce–O1	332.9(3)				∅ 152.1		
	∅ 276.0						

Table 4. Interatomic distances (pm) calculated with the single crystal lattice parameters of δ-Ce(BO₂)₃ with estimated standard deviations in parentheses.

Table 5. Interatomic angles (°) calculated with the single crystal lattice parameters of δ-Ce(BO₂)₃ with estimated standard deviations in parentheses.

O5–B1–O2 100.5(2)	O3–B2–O6 107.1(3)	O5–B3–O1 102.9(2)
O3–B1–O5 109.7(3)	O6–B2–O1 107.1(2)	O5–B3–O6 107.1(2)
O3–B1–O1 110.6(2)	O3–B2–O1 107.0(2)	O4–B3–O6 108.9(2)
O3–B1–O2 110.5(3)	O2–B2–O1 107.8(3)	O6–B3–O1 110.4(2)
O2–B1–O1 112.4(2)	O2–B2–O6 111.0(3)	O4–B3–O1 110.7(2)
O5–B1–O1 112.6(2)	O2–B2–O3 116.4(2)	O4–B3–O5 116.5(3)
∅ 109.4	∅ 109.4	∅ 109.4

Ce(BO₂)₃ was refined with full-matrix least-squares methods on F^2 with anisotropic displacement parameters for all atoms using SHELXL-97 [44]. The final difference Fourier synthesis did not reveal any significant residual peaks (see Table 1). The details of the single crystal structure measurement are shown in Table 1. Additionally, the positional parameters (Table 2), anisotropic displacement parameters (Table 3), interatomic distances, and angles (Tables 4 and 5) are listed.

Further details of the crystal structure investigation may be obtained from the Fachinformationszentrum (FIZ) Karlsruhe, D-76344 Eggenstein-Leopoldshafen, Germany (fax: (+49)7247-808-666; e-mail: crysdata@fiz-karlsruhe.de), on quoting the depository number CSD-417721.

Results and Discussion

The crystal structure of δ-Ce(BO₂)₃ is built up exclusively from $[BO_4]^{5-}$ tetrahedra, which are linked
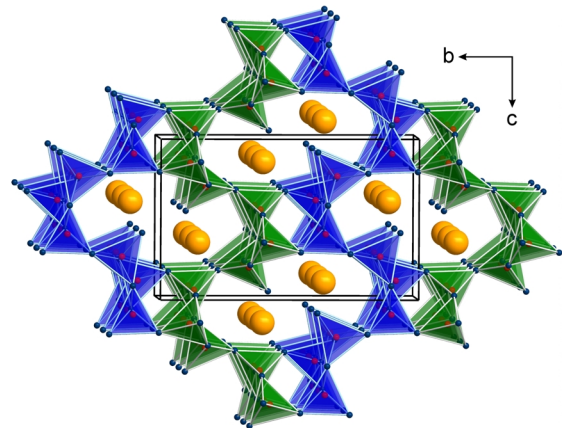

Fig. 1 (colour online). Crystal structure of δ-Ce(BO₂)₃ (view along [100]). The $[BO_4]^{5-}$ tetrahedra form a network with the cerium ions in channels along [100].

via common corners to form a network. Fig. 1 gives a view of the crystal structure along [100], showing large ten-membered rings occupied by the cerium ions, and small, empty four-membered rings. For a more detailed description of the structure, including an analysis of the main building block and its linkage to corrugated layers, which are connected to the network structure, the reader is referred to the description of the isotypic compound δ-La(BO₂)₃ (ref. [34]). In this paper, we briefly summarize the differences of the

Table 6. Charge distribution in δ-Ce(BO$_2$)$_3$, calculated with the bond-length / bond-strength (ΣV) [49, 50] and the CHARDI concept (ΣQ) [51].

	Ce	B1	B2	B3	O1	O2	O3	O4	O5	O6
ΣQ	+2.94	+3.02	+3.02	+3.02	−1.79	−2.03	−2.06	−2.03	−2.07	−2.02
ΣV	+2.89	+3.10	+3.09	+3.00	−2.04	−2.02	−2.03	−1.90	−2.04	−1.99
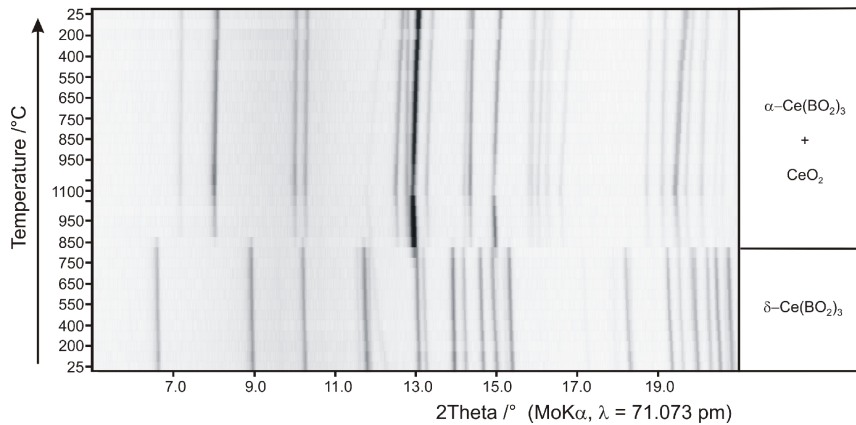
Fig. 2. *In situ* temperature-programmed X-ray powder diffraction patterns of the transformation of δ-Ce(BO$_2$)$_3$ into the normal pressure modification α-Ce(BO$_2$)$_3$ at a temperature of 850 – 900 °C.

cerium compound, due to the smaller size of Ce^{3+} (radius = 148 pm for a 12 fold coordination [45]), in comparison to La^{3+} (radius = 150 pm for coordination number 12 [45]). Inside the framework of [BO$_4$]$^{5-}$ tetrahedra, the B–O distances of the three crystallographically different [BO$_4$]$^{5-}$ groups vary between 143 and 154 pm (Table 4). The three largest values 149.9(4), 153.1(4), and 153.4(4) pm are the three B–O distances around the threefold coordinated oxygen atom O1, which are significantly longer than to the twofold coordinated oxygen atoms. Summing up, the B–O bond lengths tally with those in δ-La(BO$_2$)$_3$. Small differences are found in the environment of the rare earth ions. For δ-La(BO$_2$)$_3$, we reported a 10+2 coordination in the range 245 – 310 pm (ten atoms) plus two oxygen atoms at a distance of 325 and 331 pm [34]. Applying the same ECoN calculations (*E*ffective *Co*ordination *N*umbers according to Hoppe [46 – 48]) to δ-Ce(BO$_2$)$_3$, we find ten oxygen atoms in the range 243 – 308 pm plus two oxygen atoms at a distance of 328 and 333 pm, *i. e.* slightly shorter values due to the smaller size of Ce^{3+} as compared to La^{3+}. Analogously to the series of lanthanum *meta*-oxoborates α-, δ-, and γ-La(BO$_2$)$_3$, in which the La^{3+} ions possess a 10-, 10+2-, and 10+5-fold coordination, δ-Ce(BO$_2$)$_3$ takes also the middle position between α- and γ-Ce(BO$_2$)$_3$. The calculated densities of α-Ce(BO$_2$)$_3$ (4.30 g cm^{-3}) [24], δ-Ce(BO$_2$)$_3$ (4.98 g cm^{-3}), and γ-Ce(BO$_2$)$_3$ (5.04 g cm^{-3}) [33] increase with the applied pressure from "ambient" *via* 3.5 GPa up to 7.5 GPa, respectively.

In analogy to δ-La(BO$_2$)$_3$, we have calculated bond valence sums for δ-Ce(BO$_2$)$_3$ with the bond-length / bond-strength [49, 50] and the CHARDI concept (*Char*ge *Di*stribution in Solids according to Hoppe [51]). Table 6 displays the results of the formal ionic charges of the atoms, which are in agreement within the limits of both concepts. Again we find that the threefold coordinated O1 in δ-Ce(BO$_2$)$_3$ displays a reduced value of −1.79 (ΣQ) in the CHARDI picture comparable to the value of −1.75 in δ-La(BO$_2$)$_3$. This deviation occurs only in the CHARDI calculation, whereas the bond-length / bond-strength value of −2.04 corresponds well to the expected one. A comparative discussion was already given in great detail for δ-La(BO$_2$)$_3$ and the corresponding oxoborates, possessing three-coordinate oxygen atoms [34].

Furthermore, we have calculated the MAPLE value (*Ma*delung *P*art of *L*attice *E*nergy according to Hoppe [46 – 48]) of δ-Ce(BO$_2$)$_3$ to compare it with the sum of the MAPLE values for the underlying binary components A-type Ce$_2$O$_3$ [52] and the high-pressure modification B$_2$O$_3$-II [53] [0.5 · Ce$_2$O$_3$ (14150 kJ mol^{-1}) + 1.5 · B$_2$O$_3$-II (21938 kJ mol^{-1})]. The deviation of the calculated value (40252 kJ mol^{-1}) for δ-Ce(BO$_2$)$_3$ amounts to +0.7 % in comparison to the MAPLE value obtained from the sum of the binary sesquioxides (39982 kJ mol^{-1}).
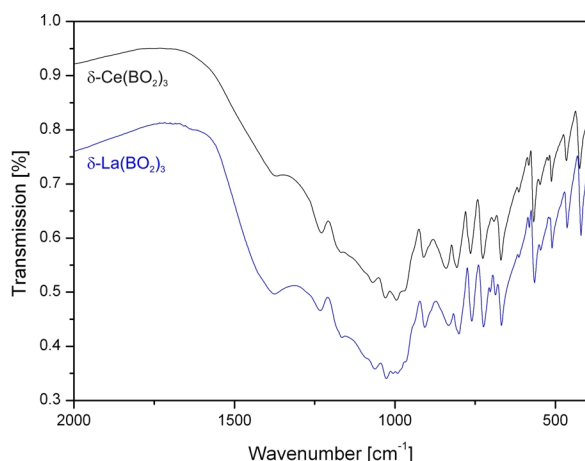
Fig. 3 (colour online). IR spectrum of δ-Ce(BO$_2$)$_3$ in comparison to the IR spectrum of the isotypic compound δ-La(BO$_2$)$_3$ [34].

Thermal behaviour of δ-Ce(BO$_2$)$_3$

The *in situ* temperature-programmed X-ray powder diffraction experiments were performed on a Stoe Stadi P powder diffractometer (MoK_α radiation) with a computer controlled Stoe furnace. The sample was enclosed into a quartz capillary and heated from r. t. up to 500 °C in steps of 100 °C, and from 500 to 1100 °C and back to 500 °C in steps of 50 °C. From 500 °C down to 100 °C, the temperature shift per range was again 100 °C. At each temperature, a diffraction pattern was recorded over the angular range $5° \leq 2\theta \leq 21°$. Fig. 2 shows that the reflections of the *meta*-oxoborate δ-Ce(BO$_2$)$_3$ can be detected up to a temperature of 850 °C. Afterwards, a transformation of the high-pressure phase δ-Ce(BO$_2$)$_3$ into the monoclinic normal-pressure *meta*-oxoborate α-Ce(BO$_2$)$_3$ occurs. Additionally, reflections of CeO$_2$ appear in the powder patterns, which result from a partial decomposition of the *meta*-oxoborates into CeO$_2$ and B$_2$O$_3$. Interestingly, the same decomposition was observed in the temperature-programmed X-ray powder diffraction experiments on the *meta*-oxoborate γ-Ce(BO$_2$)$_3$ [33].

Infrared spectroscopy of δ-Ce(BO$_2$)$_3$

An infrared (IR) spectrum of δ-Ce(BO$_2$)$_3$ (Fig. 3) was recorded on a Bruker IFS66/v spectrometer, scan-ning a range from 400 to 4000 cm^{-1}. The sample was thoroughly mixed with dried KBr (5 mg sample, 500 mg KBr) in a glove box under dried argon atmosphere. Fig. 3 shows the section 400 – 2000 cm^{-1} of the infrared spectrum of δ-Ce(BO$_2$)$_3$ in direct comparison with the spectrum of the isotypic δ-La(BO$_2$)$_3$. The spectrum of δ-Ce(BO$_2$)$_3$ is nearly identical to the spectrum of δ-La(BO$_2$)$_3$ with a slight shift to higher wavenumbers. The assignment of the absorption peaks corresponds to the situation in δ-La(BO$_2$)$_3$ (between 790 and 1150 cm^{-1}: absorptions of the tetrahedral borate group [BO$_4$]$^{5-}$ [54 – 56]; between 1300 and 1400 cm^{-1}, around 1200 cm^{-1}, and below 790 cm^{-1}: absorptions of the [OB$_3$]$^{7+}$ vibrations [11, 13, 31, 33]). For a detailed discussion of the assignment see reference [34].

Conclusions

The successful syntheses of δ-La(BO$_2$)$_3$ (5.5 GPa) and the isotypic cerium *meta*-oxoborate δ-Ce(BO$_2$)$_3$ at a pressure of 3.5 GPa have suggested that the same synthetic conditions applied to the next smaller rare earth ion Pr^{3+} could lead to an isotypic praseodymium *meta*-oxoborate. However, experiments with Pr$_6$O$_{11}$ as the rare earth oxide did not lead to the expected borate δ-Pr(BO$_2$)$_3$. Instead, the synthesis resulted in a new composition Pr$_4$B$_{10}$O$_{21}$, in which nine boron atoms possess a tetrahedral and one boron atom a trigonal coordination [57]. Obviously, there exist further unknown compositions and structures in rare earth oxoborate chemistry, which can be reached synthetically only *via* the parameter pressure.

[1] H. Huppertz, B. von der Eltz, *J. Am. Chem. Soc.* **2002**, *124*, 9376.
[2] H. Huppertz, *Z. Naturforsch.* **2003**, *58b*, 278.
[3] H. Huppertz, H. Emme, *J. Phys.: Condens. Matter* **2004**, *16*, S1283.
[4] H. Emme, H. Huppertz, *Z. Anorg. Allg. Chem.* **2002**, *628*, 2165.
[5] H. Emme, H. Huppertz, *Chem. Eur. J.* **2003**, *9*, 3623.
[6] H. Emme, H. Huppertz, *Acta Crystallogr.* **2005**, *C61*, i29.
[7] H. Emme, M. Valldor, R. Pöttgen, H. Huppertz, *Chem. Mater.* **2005**, *17*, 2707.
[8] J. S. Knyrim, H. Huppertz, *J. Solid State Chem.* **2007**, *180*, 742.
[9] J. S. Knyrim, F. M. Schappacher, R. Pöttgen, J. Schmedt auf der Günne, D. Johrendt, H. Huppertz, *Chem. Mater.* **2007**, *19*, 254.
[10] H. Huppertz, B. von der Eltz, R.-D. Hoffmann, H. Piotrowski, *J. Solid State Chem.* **2002**, *166*, 203.
[11] H. Huppertz, *Z. Naturforsch.* **2003**, *58b*, 257.
[12] H. Emme, M. Weil, H. Huppertz, *Z. Naturforsch.* **2005**, *60b*, 815.
[13] H. Huppertz, G. Heymann, *Solid State Sci.* **2003**, *5*, 281.
[14] L. Li, G. Li, Y. Wang, F. Liao, J. Lin, *Inorg. Chem.* **2005**, *44*, 8243.
[15] J. S. Knyrim, P. Becker, D. Johrendt, H. Huppertz, *Angew. Chem. Int. Ed.* **2006**, *45*, 8239.
[16] I. V. Tananaev, B. F. Dzhurinskii, B. F. Chistova, *Inorg. Mater.* **1975**, *11*, 69.
[17] I. V. Tananaev, B. F. Dzhurinskii, B. F. Chistova, *Izv. Akad. Nauk SSSR Neorg. Mater.* **1975**, *11*, 86.
[18] H. U. Bambauer, J. Weidelt, J.-S. Ysker, *Z. Kristallogr.* **1969**, *130*, 207.
[19] I. V. Tananaev, B. F. Dzhurinskii, I. M. Belyakov, *Izv. Akad. Nauk SSSR Neorg. Mater.* **1966**, *2*, 1791.
[20] G. Canneri, *Gazz. Chim. Ital.* **1926**, *56*, 450.
[21] J. Weidelt, *Z. Anorg. Allg. Chem.* **1970**, *374*, 26.
[22] J.-S. Ysker, W. Hoffmann, *Naturwissenschaften* **1970**, *57*, 129.
[23] G. K. Abdullaev, K. S. Mamedov, G. G. Dzhfarov, *Sov. Phys. Crystallogr.* **1981**, *26*, 473.
[24] F. Goubin, Y. Montardi, P. Deniard, X. Rocquefelte, R. Brec, S. Jobic, *J. Solid State Chem.* **2004**, *177*, 89.
[25] C. Sieke, T. Nikelski, Th. Schleid, *Z. Anorg. Allg. Chem.* **2002**, *628*, 819.
[26] V. I. Pakhomov, G. B. Sil'nitskaya, A. V. Medvedev, B. F. Dzhurinskii, *Inorg. Mater.* **1972**, *8*, 1107.
[27] H. Müller-Bunz, T. Nikelski, Th. Schleid, *Z. Naturforsch.* **2003**, *58b*, 375.
[28] G. K. Abdullaev, K. S. Mamedov, G. G. Dzhfarov, *Sov. Phys. Crystallogr.* **1975**, *20*, 161.
[29] A. Goriounova, P. Held, P. Becker, L. Bohatý, *Acta Crystallogr.* **2003**, *E59*, i83.
[30] T. Nikelski, Th. Schleid, *Z. Anorg. Allg. Chem.* **2003**, *629*, 1017.
[31] H. Emme, T. Nikelski, Th. Schleid, R. Pöttgen, M. H. Möller, H. Huppertz, *Z. Naturforsch.* **2004**, *59b*, 202.
[32] H. Emme, C. Despotopoulou, H. Huppertz, *Z. Anorg. Allg. Chem.* **2004**, *630*, 1717.
[33] H. Emme, C. Despotopoulou, H. Huppertz, *Z. Anorg. Allg. Chem.* **2004**, *630*, 2450.
[34] G. Heymann, T. Soltner, H. Huppertz, *Solid State Sci.* **2006**, *8*, 821.
[35] V. F. Ross, J. O. Edwards, *The Structural Chemistry of the Borates*, Wiley, New York, **1967**.
[36] D. Walker, M. A. Carpenter, C. M. Hitch, *Am. Mineral.* **1990**, *75*, 1020.
[37] D. Walker, *Am. Mineral.* **1991**, *76*, 1092.
[38] H. Huppertz, *Z. Kristallogr.* **2004**, *219*, 330.
[39] J.-Y. Henry, *Mater. Res. Bull.* **1976**, *11*, 577.
[40] R. Böhlhoff, H. U. Bambauer, W. Hoffmann, *Z. Kristallogr.* **1971**, *133*, 386.
[41] J. W. Visser, *J. Appl. Crystallogr.* **1969**, *2*, 89.
[42] WinX^{POW} Software, Stoe & Cie GmbH, Darmstadt (Germany) **1998**.
[43] W. Herrendorf, H. Bärnighausen, HABITUS, Universities of Karlsruhe and Giessen (Germany) **1993/1997**.
[44] G. M. Sheldrick, SHELXL-97, Program for the Refinement of Crystal Structures, University of Göttingen, Göttingen (Germany) **1997**.
[45] R. D. Shannon, *Acta Crystallogr.* **1976**, *A32*, 751.
[46] R. Hoppe, *Angew. Chem.* **1966**, *78*, 52.
[47] R. Hoppe, *Angew. Chem.* **1970**, *82*, 7.
[48] R. Hübenthal, MAPLE, Program for the Calculation of MAPLE Values, Vers. 4, University of Giessen (Germany) **1993**.
[49] I. D. Brown, D. Altermatt, *Acta Crystallogr.* **1985**, *B41*, 244.
[50] N. E. Brese, M. O'Keeffe, *Acta Crystallogr.* **1991**, *B47*, 192.
[51] R. Hoppe, S. Voigt, H. Glaum, J. Kissel, H. P. Müller, K. J. Bernet, *J. Less-Common Met.* **1989**, *156*, 105.
[52] N. Hirosaki, S. Ogata, C. Kocer, *J. Alloys Compd.* **2003**, *351*, 31.
[53] C. T. Prewitt, R. D. Shannon, *Acta Crystallogr.* **1968**, *B41*, 244.
[54] M. Ren, J. H. Lin, Y. Dong, L. Q. Yang, M. Z. Su, L. P. You, *Chem. Mater.* **1999**, *11*, 1576.
[55] J. P. Laperches, P. Tarte, *Spectrochim. Acta* **1966**, *22*, 1201.
[56] G. Blasse, G. P. M. van den Heuvel, *Phys. Stat. Sol.* **1973**, *19*, 111.
[57] A. Haberer, G. Heymann, H. Huppertz, *J. Solid State Chem.* **2007**, *180*, doi:10.1016/j.jssc.2007.02.021.